Available online at www.sciencedirect.com
ScienceDirect
Bioorganic & Medicinal Chemistry Letters 19 (2009) 1030–1034
Bioorganic & Medicinal Chemistry Letters

Development of pH-responsive core–shell nanocarriers for delivery of therapeutic and diagnostic agents

Shangjie Xu,[a] Ying Luo,[a] Ralph Graeser,[b] André Warnecke,[b] Felix Kratz,[b] Peter Hauff,[c] Kai Licha[c] and Rainer Haag[a,*]

[a]*Institut für Chemie und Biochemie, Freie Universität Berlin, Takustrasse 3, 14195 Berlin, Germany*
[b]*Tumor Biology Center, Breisacher Strasse 117, 79106 Freiburg, Germany*
[c]*Bayer Schering Pharma AG, Global Drug Discovery, Müllerstr. 170, 13342 Berlin, Germany*

Received 5 December 2007; revised 9 January 2008; accepted 12 January 2008
Available online 18 January 2008

Abstract—In this paper new dendritic core–shell architectures with pH-labile linkers based on hyperbranched polyglycerol cores and biocompatible poly(ethylene glycol) shells were synthesized which encapsulate the anticancer agent doxorubicin and a dye for near-infrared imaging, an indotricarbocyanine. Acid-sensitive properties of the new nanocarriers and in vitro cytotoxicity of the doxorubicin-nanocarrier are presented as well as preliminary data regarding their toxicity and tumor targeting potential in nude mice.

Most clinically used anticancer drugs are low-molecular weight compounds that diffuse rapidly into healthy tissues and are distributed evenly within the body resulting in the common and often severe side effects associated with these agents. An attractive solution to reduce such side effects is the development of macromolecular prodrugs[1] or drug-delivery systems in which the drug molecules are physically encapsulated in nanoparticles, micelles or liposomes.[2,3] Macromolecular drug-delivery systems can selectively accumulate in solid tumors due to passive targeting, a phenomenon circumscribed by the enhanced permeability and retention (EPR) effect.[4]

Blood vessels in most normal tissues have an intact endothelial layer which allows the diffusion of small molecules but excludes macromolecules or other nanoparticles from the tissue. In contrast, as a consequence of its fast growth, the endothelial layer of blood vessels in tumor tissue is often porous, and both small and large molecules have access to the malignant tissue. Due to the lack of a lymphatic drainage system in tumor tissue, macromolecules are retained and accumulate in tumor tissue.[4]

Physical aggregates such as liposomes and micelles have been frequently used as drug-delivery systems in the past decades.[3] However, they have a limited stability under shear force and other environmental effects, such as temperature, pressure, and dilution in the body due to their non-covalent assembly.[5] Therefore, polymer-based nanocarrier systems have gained interest for targeted delivery of drugs.[2,6] The covalent immobilization of dendrimers with an appropriate shell results in stable core–shell architectures that are suitable for the non-covalent encapsulation of guest molecules.[7–16] Meijer and Kono have reported on water-soluble core–shell architectures for the encapsulation of dyes and drugs.[17,18] Moreover, the size of these dendritic nanoparticles can be exactly defined in the range of 3–10 nm, and delivery systems in this size-range have shown effective accumulations in tumor tissues.[19–21]

For effective release of the drug at the tumor site, both the acidic pH in tumor tissue and in endosomes or lysosomes can be exploited, a strategy that has often aided the design of macromolecular prodrugs.[1,22] Based on the pioneering work of Otto Warburg, who described cancer cells that convert glucose to lactate even in non-hypoxic conditions thus lowering the pH-value of the tumor environment,[23] non-invasive techniques with

Keywords: Dendritic core–shell architectures; pH-labile linkers; Hyperbranched polyglycerol; Biocompatible polymers; Anticancer agent; Tumor diagnostic; In vitro cytotoxicity; Tumor targeting mouse model.
* Corresponding author. Tel./fax: +49 30 838 52633; e-mail: haag@chemie.fu-berlin.de

0960-894X/$ - see front matter © 2008 Elsevier Ltd. All rights reserved.
doi:10.1016/j.bmcl.2008.01.043

pH-electrodes have demonstrated that the pH-value in tumor tissue is often 0.5–1.0 units lower than in normal tissue.[24] This pH-shift, although small, could contribute to the extracellular acid-sensitive release of drugs, especially if the drug-delivery system remains in the tumor interstitium for longer periods of time.

A larger pH shift from 7.2–7.4 in the blood or extracellular spaces to 4.0–6.5 in the various intracellular compartments takes place during cellular uptake of macromolecules. The significant drop in the pH-value is a unique physical property in living systems that can be exploited for intracellular drug delivery by coupling drugs to suitable carriers through acid-sensitive bonds.

Consequently, we set out to develop a general synthetic concept for building water-soluble dendritic architectures for application in pH-dependent release of the encapsulated guest by formation of imine bonds between the core and the shell.

Hyperbranched polyglycerol (PG) was used as the dendritic core which can be obtained with defined molecular weight (M_n = 10,000 g/mol, PDI = 2.0). Poly(ethylene glycol) monomethyl ether (mPEG) chains were used as the shell component to render water-solubility, to minimize the immunogenic potential and to increase the blood circulation half-life of the resulting nanocarriers considering that this strategy has proven successful in the development of Stealth-liposomes.[3] The dendritic nanocarriers were prepared by attaching tri-PEGylated benzaldehydes of varying lengths (n = 4, 7, 15, 24) to the polyglycerol amine through an imine bond in a mixture of methanol and chloroform as shown in Figure 1 (see Note 1).

The tri-PEGylated benzaldehydes with different lengths of PEG chains that form the shell of the nanocarrier were prepared in multi-step syntheses as previously described for hyperbranched polyethyleneimine.[25,26] Figure 1 depicts an idealized nanocarrier with an almost complete shell. In fact, the degree of functionality (DF = number of shell molecule/number of terminal NH_2 units of PG, given in %) of the obtained nanocarriers **N1**–**N4** varied (DF value between 35 and 67) as determined by integration of the respective ^{1}H NMR signals.[15] Using larger PEG chains, the DF decreased significantly probably due to their steric hindrance. The formation of the core–shell architectures was confirmed by IR spectroscopy, in which the peaks of C=O bonds, at about 1695 cm^{-1}, disappeared and the peaks responsible for C=N bonds, at about 1645 cm^{-1} for nanocarriers **N1**–**N4**, were observed. Alternatively, the formation of imine bonds was confirmed by ^{1}H NMR spectra, in which the signals of aldehyde protons, at about 9.80 ppm for building block, tri-PEGylated benzaldehydes, disappeared and the corresponding signals of the imines at 7.8–8.1 ppm for **N1**–**N4** were observed.

It is well known that aromatic imine bonds are sensitive to pH changes in the range of pH 5–6. The acid-sensitivity of the imine bond for nanocarrier **N1** was examined in a biphasic system using IR spectroscopy (see Note 2). The nanocarrier was dissolved in chloroform and a solution of phosphate–citric acid buffer at pH 5.0 or 7.4. Samples were taken over 1000 min and the appearance of a carbonyl band at 1695 cm^{-1} used to confirm the cleavage of the imine bond (see Fig. 2) resulting in a half-life for the imine bond of 80 min at pH 5, and of 480 min at pH 7.4.

In a next step, we investigated the encapsulation of the anticancer agent doxorubicin and a near-infrared (NIR) dye for optical imaging (see Fig. 3).[27] The compounds were incubated with **N1**–**N4** in aqueous media for 16 h at room temperature and the rate of encapsulation estimated by size-exclusion chromatography demonstrating that the nanocarrier with the shortest PEG chain (**N1**, n = 4) showed good encapsulation efficiency. Experiments with varying ratios of drug (dye)/nanocarrier showed that up to 5 molecules of doxorubicin or NIR dye were associated with **N1** (preparation of the dye/drug nanocarriers is summarized in Note 3).

The pH-dependent release of the doxorubicin-nanocarrier was investigated by incubation at pH 4.0 or 7.4 (37 °C) and dialyzing a sample over time with a Mirocon YM-10 (cut-off MW 10,000 Da) and determining the amount of released doxorubicin in the ultrafiltrate by HPLC (see Note 4). After 4 h, ~20% released doxorubicin was determined at pH 4.0, but only ~10% at pH 7.4. However, after 16 h the amount of released doxorubicin at both pH 4.0 and 7.4 was ~20% with no further release of doxorubicin even after 48 h. These data show that a certain fraction of doxorubicin can be released in a pH-dependent manner, but the major amount of the drug remains associated with the nanocarrier under the chosen experimental conditions.

Cytotoxicity experiments with the doxorubicin-nanocarrier in three cancer cell lines demonstrated much higher IC_{50} values in the micromolar range (3.3–31 μM) than for free doxorubicin (0.02–0.39 μM) (Table 1), suggesting that the doxorubicin-nanocarrier exhibited much lower antiproliferative activity than free doxorubicin. The results taken together imply that the architecture of the nanocarrier needs to be improved to enable a complete release of the encapsulated doxorubicin.

In order to assess the toxicity and tumor targeting properties of these nanocarrier systems we performed some initial in vivo experiments. In an orientating study in nude mice the doxorubicin-nanocarrier could be dosed up to 24 mg/kg doxorubicin equivalents as an intravenous injection (see Table 2) which is a significant increase in the maximum tolerated dose (MTD) compared to free doxorubicin (MTD).[28] This in vivo experiment also shows that there is no acute toxicity of the nanocarrier at these doses.

The ability of the nanocarriers to localize in tumors in vivo was preliminarily assessed by fluorescence imaging of tumor-bearing mice using an established imaging set-up.[29] After intravenous injection of the nanocarrier **N1** loaded with a hydrophilic cyanine

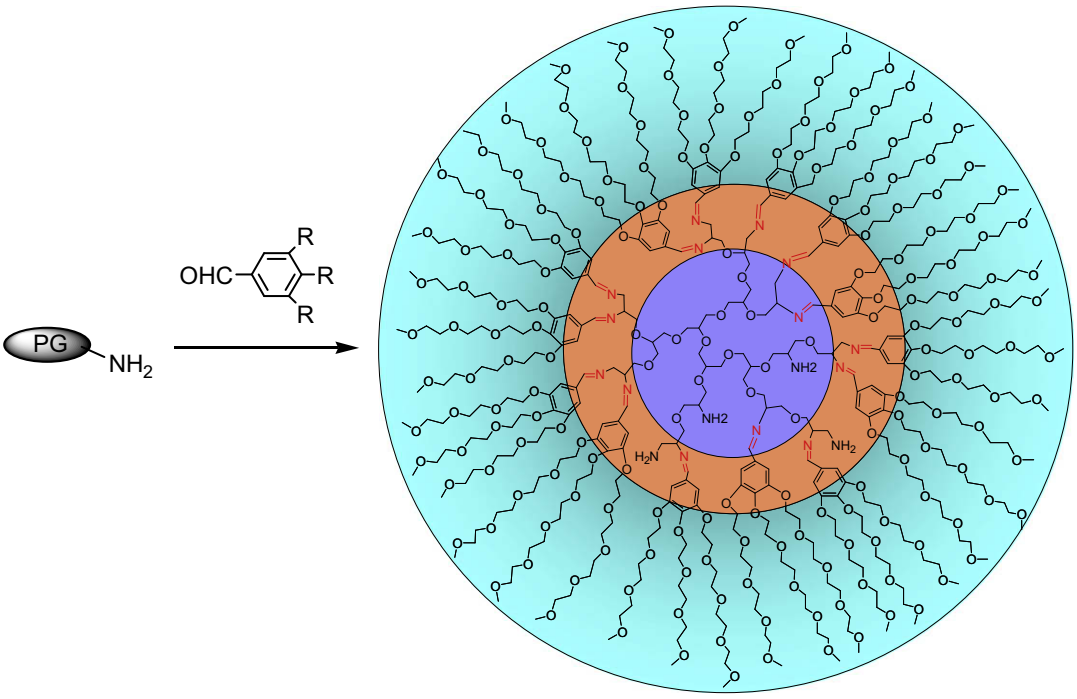

Figure 1. Synthesis of pH-labile dendritic core–shell architectures and structure of a small idealized fragment of the core–shell architecture **N1** with R = $O(CH_2CH_2O)_nCH_3$, **N1**–**4**: n = 4, 7, 16, and 24, respectively.

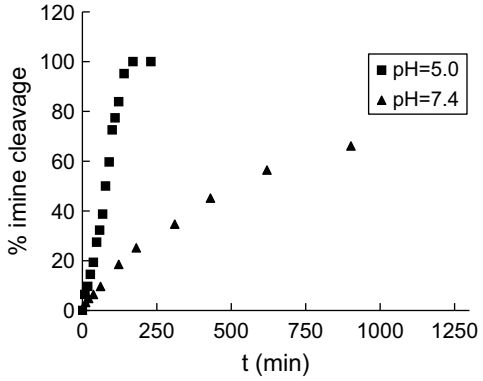

Figure 2. The amount of cleaved imine bonds as determined by IR signals for nanocarriers at different pH-values.

Table 1. IC_{50} values of doxorubicin and the doxorubicin-nanocarrier **N1** in two pancreas carcinoma and one mamma carcinoma cell line

Cell line	IC_{50} value doxorubicin (μM)	IC_{50} value doxorubicin-nanocarrier (μM)
Pancreas AsPC1 LN[a]	0.39	31
Pancreas MIA-PaCa2 ELN[a]	0.02	19
MDA-MB 231[b]	0.22	3.3

[a] For IC_{50} measurements, 0.2×10^4 cells were plated per well in a 96-well plate. After 24 h, serial dilutions of the drugs were added in triplicates. Cells were incubated for 72 h and then lysed in 100 μL of luciferase assay buffer, and 10 μL of the lysate were assayed for luciferase activity.

[b] For IC_{50} measurements, 0.2×10^4 cells were plated per well in a 96-well plate. After 24 h, serial dilutions of the drugs were added in triplicates. Alamar blue was added to the medium after 69 h, and the cells were incubated for another 3 h, before the fluorescence was measured at 590 nm.

dye (dye dose 2.5 μmol/kg) whole body fluorescence images at different time points were acquired. A preferential uptake with a maximum of tumor-to-normal tissue contrast at 6 h post injection could be demonstrated (see Fig. 3). Increased levels of tissue fluorescence suggest that the nanocarrier alters the biodistribution of the free dye leading to higher concentrations in the nanocarrier format.

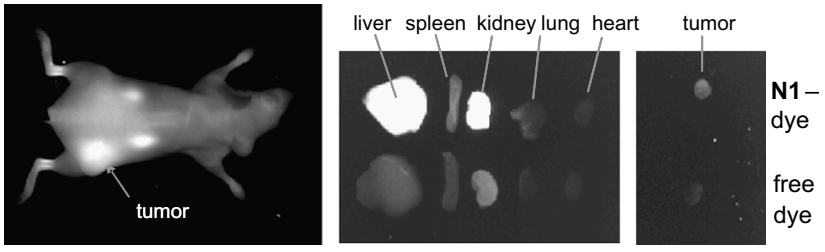

Figure 3. Fluorescence images of tumor-bearing mouse (F9 teratocarcinoma) 6 h after iv injection of nanocarrier **N1**/dye (1:5) at a dye dose of 2.5 μmol/kg, and organ preparations of animals injected with free dye and nanocarrier **N1**/dye (6 h), laser excitation at 740 nm, image acquisition with CCD-camera above 780 nm.

Table 2. Orientating toxicity study with the doxorubicin-nanocarrier **N1**

Dose doxorubicin-nanocarrier (in doxorubicin equivalents)[a] (mg/kg)	Toxic deaths	Body weight change (BWC %)
4	0	0
8	0	−2
16	0	−9
24	0	−16

[a] The doxorubicin-nanocarrier was injected intravenously to one female NMRI: nu/nu mouse per dose. Mice were held in individually ventilaged cages under sterile and standardized environmental conditions (25 ± 2 °C room temperature, 50 ± 10% relative humidity, 12 h light-dark-rhythm). They received autoclaved food and bedding (ssniff, Soest, Germany) and acidified (pH 4.0) drinking water ad libitum. All animal experiments were performed under the auspices of the German Animal Protection Law.

In summary, we have developed a new dendritic core–shell system with acid-sensitive properties that is water-soluble, shows adequate systemic tolerability and demonstrates tumor targeting potential. Encapsulation with polar NIR dyes and anticancer drugs such as doxorubicin was successfully demonstrated. Although an acid-sensitive release of doxorubicin from the doxorubicin-nanocarrier could be shown, drug release was incomplete and needs to be improved in further work.

Acknowledgments

We thank the Ministry of Science for their continuing support of this work for a NanoFutur award for R. Haag and F. Kratz (BMBF 03X5501).

References and notes

1. Kratz, F.; Muller, I. A.; Ryppa, C.; Warnecke, A. *ChemMedChem* **2007**, *3*, 20.
2. Haag, R.; Kratz, F. *Angew. Chem. Int. Ed.* **2006**, *45*, 1198.
3. Allen, T. M.; Cullis, P. R. *Science* **2004**, *303*, 1818.
4. Maeda, H. *Adv. Enzyme Regul.* **2001**, *41*, 189.
5. Jones, M. C.; Ranger, M.; Leroux, J. C. *Bioconjugate Chem.* **2003**, *14*, 774.
6. Duncan, R. *Nat. Rev. Drug Discov.* **2003**, *2*, 347.
7. Zeng, F. W.; Zimmerman, S. C. *Chem. Rev.* **1997**, *5*, 1681.
8. Liu, M.; Fréchet, J. M. J. *Pharm. Sci. Technol. Today* **1999**, *2*, 393.
9. Liu, M.; Kono, K.; Fréchet, J. M. J. *J. Polym. Sci. Polym. Chem.* **1999**, *37*, 3492.
10. Liu, M.; Kono, K.; Fréchet, J. M. J. *J. Control. Release* **2000**, *65*, 121.
11. Baars, M. W. P. L.; Meijer, E. W. *Top. Curr. Chem.* **2000**, *210*, 131.
12. Vögtle, F.; Gestermann, S.; Hesse, R.; Schwierz, H.; Windisch, B. *Prog. Polym. Sci.* **2000**, *25*, 987.
13. Esfand, R.; Tomalia, D. A. *Drug Discov. Today* **2001**, *6*, 427.
14. Zimmerman, S. C.; Lawless, L. J. *Top. Curr. Chem.* **2001**, *217*, 95.
15. Krämer, M.; Stumbé, J. F.; Türk, H.; Krause, S.; Komp, A.; Delineau, L.; Prokhorova, S.; Kautz, H.; Haag, R. *Angew. Chem. Int. Ed.* **2002**, *41*, 4252.
16. Stiriba, S. E.; Frey, H.; Haag, R. *Angew. Chem. Int. Ed.* **2002**, *41*, 1329.
17. Baars, M. W. P. L.; Kleppinger, R.; Koch, M. H. J.; Yeu, S. L.; Meijer, E. W. *Angew. Chem. Int. Ed.* **2000**, *39*, 1285.
18. Kojima, C.; Kono, K.; Maruyama, K.; Takagishi, T. *Bioconjugate Chem.* **2000**, *11*, 910.
19. Duncan, R. *Anti-cancer Drug* **1992**, *3*, 175.
20. Maeda, H.; Seymour, L. W.; Miyamoto, Y. *Bioconjugate Chem.* **1992**, *3*, 351.
21. Kataoka, K.; Kwon, G. S.; Yokoyama, M.; Okano, T.; Sakurai, Y. *J. Control. Release* **1993**, *24*, 119.
22. Kratz, F.; Beyer, U.; Schütte, M. T. *Crit. Rev. Ther. Drug Carrier Syst.* **1999**, *16*, 245.
23. Warburg, O. *Science* **1956**, *124*, 269.
24. Tannock, I. F.; Rotin, D. *Cancer Res.* **1989**, *49*, 4373.
25. Xu, S.; Luo, Y.; Haag, R. *Macromol. Biosci.* **2007**, *7*, 968.
26. Xu, S.; Luo, Y.; Haag, R. *Macromol. Rapid Commun.* **2008**, *29*, 171.
27. Licha, K.; Olbrich, C. *Adv. Drug Delivery Rev.* **2005**, *57*, 1087.
28. Bertazzoli, C.; Rovero, C.; Ballerini, B.; Lux, B.; Balconi, F.; Antongiovanni, V.; Magrini, U. *Toxicol. Appl. Pharm.* **1985**, *79*, 412.
29. Perlitz, C.; Licha, K.; Scholle, F. D.; Ebert, B.; Bahner, M.; Hauff, P.; Moesta, K. T.; Schirner, M. *J. Fluoresc.* **2005**, *15*, 443.
30. Sunder, A.; Hanselmann, R.; Frey, H.; Mülhaupt, R. *Macromolecules* **1999**, *32*, 4240.
31. Haag, R.; Mecking, S.; Türk, H. Patent Application DE10211664A1, 2002.
32. Roller, S.; Zhou, H.; Haag, R. *Mol. Divers.* **2005**, *9*, 305.

Note 1. *Synthesis of the nanocarriers **N1**–**N4**:* Polyglycerol (M_n = 10,000 g/mol, PD = 2.0) was prepared according to published procedures.[30,31] Polyglycerol amine (DF = 82%) was prepared as described previously.[32] The tri-PEGylated benzaldehydes with different lengths of PEG chains that form the shell of the nanocarrier were prepared in multi-step syntheses as previously described.[25,26] The benzoylated dialysis tubing with average flat width of 32 mm was obtained from Sigma–Aldrich.

General procedure: To a solution of polyglycerol amine (2 mmol $-NH_2$) in methanol (20 mL) tri-PEGylated benzaldehyde (1 equiv) dissolved in methanol (20 mL) was added dropwise at room temperature during 4 h. The solvent was removed and the crude product was further purified via dialysis in methanol for 48 h and the methanol was then removed in high vacuum to yield the final products **N1**–**N4**.

*Data for **N1**:* ^{1}H NMR (250 MHz, $CDCl_3$): δ (ppm) = 3.2–3.3 [PG–N=CH-aryl–(O–(CH$_2$–CH$_2$–O)$_4$–CH_3)$_3$], 3.5–3.9 [*PG*–N=CH-aryl–(O–CH$_2$–CH_2–O–(CH_2–CH_2–O)$_3$–CH$_3$)$_3$], 4.0–4.1 [PG–N=CH-aryl–(O–CH_2–CH$_2$–O–(CH$_2$–CH$_2$–O)$_3$–CH$_3$)$_3$], 6.7–7.9 [PG–N=CH-*aryl*–(O–CH$_2$–CH$_2$–O–(CH$_2$–CH$_2$–O)$_3$–CH$_3$)$_3$], 7.9–8.1 [PG–N=C*H*-aryl–(O–CH$_2$–CH$_2$–O–(CH$_2$–CH$_2$–O)$_3$–CH$_3$)$_3$]; ^{13}C NMR (63 MHz, $CDCl_3$): δ (ppm) = 58.95 [PG–N=CH-aryl–(O–(CH$_2$–CH$_2$–O)$_4$–*C*H$_3$)$_3$], 68.90–72.44 [*PG*–N=CH-aryl–*TTEG*], 107.41–153.04 [PG–N=CH-*aryl*–(O–(CH$_2$–CH$_2$–O)$_4$–CH$_3$)$_3$], 162.01 [PG–N=*C*H-aryl–(O–(CH$_2$–CH$_2$–O)$_4$–CH$_3$)$_3$]; IR: ν (cm^{-1}) = 1645.1 (C=N).

*Data for **N2**:* ^{1}H NMR (250 MHz, $CDCl_3$): δ (ppm) = 3.2–3.3 [PG–N=CH-aryl–(O–$(CH_2–CH_2–O)_7$–$CH_3)_3$], 3.4–3.9 [*PG*–N=CH-aryl–(O–CH_2–CH_2–O–$(CH_2–CH_2–O)_6$– $CH_3)_3$], 4.0–4.2 [PG–N=CH-aryl–(O–CH_2–CH_2–O–$(CH_2–CH_2–O)_6$–$CH_3)_3$], 6.5–7.0 [PG–N=CH-*aryl*–(O–CH_2–CH_2–O–$(CH_2–CH_2–O)_6$–$CH_3)_3$], 7.9–8.1 [PG–N=C*H*-aryl–(O–CH_2–CH_2–O–$(CH_2–CH_2–O)_6$–$CH_3)_3$]; ^{13}C NMR (63 MHz, $CDCl_3$): δ (ppm) = 58.93 [PG–N=CH-aryl–(O–$(CH_2–CH_2–O)_7$–$CH_3)_3$], 69.60–71.90 [*PG*-N=CH-aryl-(O–(CH_2–CH_2–$O)_7$–$CH_3)_3$], 107.30–153.00 [PG–N=CH-*aryl*–(O–$(CH_2–CH_2–O)_7–CH_3)_3$], 178.49 [PG–N=*C*H-aryl–(O–$(CH_2–CH_2–O)_7–CH_3)_3$]; IR: ν (cm^{-1}) = 1645.6 (C=N).

*Data for **N3**:* ^{1}H NMR (250 MHz, $CDCl_3$): δ (ppm) = 3.3 [PG–N=CH-aryl–(O–$(CH_2–CH_2–O)_{16}$–$CH_3)_3$], 3.4–3.9 [*PG*–N=CH-aryl–(O–CH_2–CH_2–O–$(CH_2–CH_2–O)_{15}$–$CH_3)_3$], 4.0–4.2 [PG–N=CH-aryl–(O–CH_2–CH_2–O–$(CH_2–CH_2–O)_{15}$–$CH_3)_3$], 6.5–7.0 [PG–N=CH-*aryl*–(O–CH_2–CH_2–O–$(CH_2–CH_2–O)_{15}$–$CH_3)_3$], 7.9–8.2 [PG–N=C*H*-aryl–(O–CH_2–CH_2–O–$(CH_2–CH_2–O)_{15}$–$CH_3)_3$]; IR: ν (cm^{-1}) = 1646.1 (C=N).

*Data for **N4**:* ^{1}H NMR (63 MHz, $CDCl_3$): δ (ppm) = 3.2–3.3 [PG–N=CH-aryl–(O–$(CH_2–CH_2–O)_{24}$–$CH_3)_3$], 3.4–3.9 [*PG*–N=CH-aryl–(O–CH_2–CH_2–O–(CH_2–CH_2–$O)_{23}$–$CH_3)_3$], 4.0–4.2 [PG–N=CH-aryl–(O–CH_2–CH_2–O–$(CH_2–CH_2–O)_{23}$–$CH_3)_3$], 6.6–7.0 [PG–N=CH-*aryl*–(O–CH_2–CH_2–O–$(CH_2–CH_2–O)_{23}$–$CH_3)_3$], 7.9–8.2 [PG–N=C*H*-aryl-(O-CH_2–CH_2–O–$(CH_2–CH_2–O)_{23}$–$CH_3)_3$]; ^{13}C NMR (250 MHz, $CDCl_3$): δ (ppm) = 58.60 [PG–N=CH-aryl–(O–$(CH_2–CH_2–O)_{24}$–$CH_3)_3$], 68.50–72.40 [*PG*–N=CH-aryl–*(O–(*CH_2–CH_2–*O)*$_{24}$–$CH_3)_3$], 107.20–152.60 [PG–N=CH-*aryl*–(O–$(CH_2–CH_2–O)_{24}–CH_3)_3$], 162.27 [PG–N=*C*H-aryl–(O–$(CH_2–CH_2–O)_{24}–CH_3)_3$]; IR: ν (cm^{-1}) = 1645.5 (C=N).

Note 2. *pH-dependent stability study of the nanocarrier **N1**:* Ten milliliters of the phosphate–citric acid buffer solutions with different pH-values (at pH 5.0 and 7.4, respectively) were stirred with 10 mL chloroform solution of the shell-functionalized dendrimers (0.1 mM). During given time intervals, 0.25 mL of the organic layer was transferred into a KBr cell and the IR spectra were measured. The absorption maximum of the tri-PEGylated benzaldehyde at 1695 cm^{-1} was plotted versus time (see Fig. 2).

Note 3. *Preparation of the doxorubicin-nanocarrier*: Forty milligrams of **N1** and 4.0 mg doxorubicin HCl were dissolved in 2.6 mL 10 mM sodium phosphate buffer/5% D-glucose buffer (pH 7.0) and addition of 40 μL 1 N NaOH and the mixture stirred for 13 h under light protection. The doxorubicin-nanocarrier was isolated over a 20 mL syringe filled with Sephadex G25 (fine) in sterile-filtered 10 mM sodium phosphate buffer/5% D-glucose buffer (pH 7.0) (height of the column 12 cm). Using Centriprep YM01 the solution is concentrated to 2.5 mL (twice at 4000 U/min for 15 min). The concentration of doxorubicin in the sample is analyzed by diluting a sample 1:40 with 1 N HCl, incubating the sample for 30 min at RT, and determining the doxorubicin concentration at 495 nm with a calibration curve (doxorubicin in 1 N HCl, 250, 125, 62.5, 31.25 μM) yielding a doxorubicin concentration of 2700 μM. The solution was stored at +4 °C.

Preparation of the nanocarrier with cyanine dye: The hydrophilic indotricarbocyanine 5,5′-sulfonato-bis-1,1′-(2-sulfonatoethyl)indotricarbocyanine, trisodium salt, was synthesized in analogy to published procedures.[29] Ten milligrams of *N1* and 1.3 mg cyanine dye were dissolved in 0.65 mL 10 mM sodium phosphate buffer/5% D-glucose buffer (pH 7.0), and the mixture was stirred for 13 h under light protection. The nanocarrier–dye complex was isolated by SEC via Sephadex G25 (fine) (height of the column 4.5 cm) with 10 mM sodium phosphate buffer/5% D-glucose buffer (pH 7.0). The concentration of dye was determined by photospectrometry (extinction coefficient of 210,000 L mol^{-1} cm^{-1} at 754 nm).

Note 4. *Determination of the pH-dependent release of doxorubicin from the doxorubicin-nanocarrier:* For determining the amount of released doxorubicin at pH 7.0 (10 mM sodium phosphate) and pH 4.0 (20 mM sodium acetate). A 1300 μM solution of the doxorubicin-nanocarrier was incubated at 37 °C and samples ultrafiltrated with Microcon utracel YM-10 (Millipore, Germany) for 30 min at 5000 rpm at 0, 4, 16, and 48 h. The doxorubicin concentration in the ultrafiltrate was determined by HPLC with a Nucleosil RP (C-18) column (EC 250/4, isocratic eluent: 70% 20 mM K_2HPO_4 (pH 7.0), 30% acetonitrile) on a Waters System (pump: Waters 616, detector: Waters 996 Photodiode Array Detector; controller: Waters 600S; auto sampler: Waters 717; Empower PDA software).